Designing a Commercial Ion-Exchange Carousel to Treat DOE Wastes Using CST Granules

M. E. Huckman, I. M. Latheef, and R. G. Anthony
Dept. of Chemical Engineering, Kinetics, Catalysis, and Reaction Engineering Group, Texas A&M University, College Station, TX 77843

A column carousel system was designed to treat nuclear waste at the Savannah River Site. A carousel model was used to simulate cesium removal in an ion-exchange carousel loaded with crystalline silicotitanate (CST) granules. The model accounts for axial dispersion and resistance to film and intraparticle diffusion. The effect of resistance to intraparticle diffusion on the required column volumes is significant. Values of the effective diffusivity of 0.25 to 0.6 $\times 10^{-10}$ m^2/s were estimated from bench-scale column experiments. This range of values resulted in a variation of column volumes by a factor of 3. The Zheng-Anthony-Miller equilibrium model was used to estimate Cs isotherms. The largest carousel volume did not result from waste with the lowest equilibrium loading. For wastes with low equilibrium loadings, the switching interval increased, which increases the volume of CST required to treat the same volume of waste.

Introduction

The Department of Energy (DOE) has been charged with remediating millions of gallons of aqueous radioactive waste. Much of this waste was produced during the Cold War and is currently contained in underground storage tanks at DOE facilities in Savannah River, Hanford, Oak Ridge, and others. To this end, the DOE is evaluating several treatment technologies. Ion exchange using the crystalline silicotitanate (CST) TAM-5, which was synthesized by Anthony et al. (1993, 1994), is currently under evaluation. UOP IONSIV IE-911, the commercially available engineered form of TAM-5, can selectively remove cesium (Cs), one of the key radioactive components (Marsh et al., 1993; Alm, 1997; Miller and Brown, 1997). The Cs-loaded CST is then converted into a nonleachable solid, which is stored in long-term geologic repositories.

A major cost of the treatment technology is expected to be the conversion and disposal of the CST. Thus, a key design consideration is to maximize Cs loading onto the CST to minimize the volume of CST, which requires a costly conversion process. Another consideration is that radioactive wastes have a variety of compositions so the design must be flexible enough to treat wastes with a wide range of compositions. This article presents the design of ion-exchange carousels to utilize CST for the treatment of wastes currently stored at the Savannah River Site. The waste compositions used for the design are based on average compositions and bounding cases as defined by SRS personnel. Bounding cases are based on the range of compositions anticipated when processing the SRS wastes. The major cases involved use average, nominally high, and bounding high Cs^+ and K^+ concentrations, and average and high OH^- and $(NO_3)^-$ concentrations. These cases are defined in Table 1 and are referred to as Avg. HiOH, and HiNO concentrations.

Correspondence concerning this article should be addressed to R. G. Anthony.

Design Equations

The equations included in the model are the bulk-liquid material balance, which includes axial dispersion and film resistance to diffusion, a two-phase homogeneous particle material balance, and an equilibrium isotherm. Previous research (Huckman et al., 1999; Latheef, 1999; Huckman, 1999) has shown that this type of model can be used to simulate fixed-bed columns using CSTs to ion exchange Cs, Sr, and Rb. The previous work also showed that the model that represents physical reality the best is a macro-micro model for resistance to intraparticle and intracrystalline diffusion. However, a major principle of design models is to use the simplest model that is practical. To this end the particles were treated as a uniform pore structure with liquid in the pore in equilibrium with the solid phase of the particle (Latheef et al., 2000).

Table 1. Molar (mol/L) Concentrations for Nominal (n) and Bounding (b) Cases of the SRS Waste Simulants

Component	Avg.-*n*.	Avg.-*b*	HiOH-*n*	HiOH-*b*	HiNO-*n*	HiNO-*b*
Na^+	5.6	5.465	5.6	5.48	5.6	5.454
Cs^+	0.00014	0.0007	0.00037	0.0007	0.00014	0.0007
K^+	0.015	0.150	0.030	0.150	0.0041	0.150
OH^-	1.91	1.91	3.05	3.05	1.17	1.17
NO_3^-	2.14	2.14	1.10	1.10	2.84	2.84
NO_2^-	0.52	0.52	0.74	0.74	0.37	0.37
$Al(OH)_4^-$	0.31	0.31	0.27	0.27	0.32	0.32
CO_3^{-2}	0.16	0.16	0.17	0.17	0.16	0.16
SO_4^{-2}	0.15	0.15	0.030	0.030	0.22	0.22
Cl^-	0.025	0.025	0.010	0.010	0.040	0.040
F^-	0.032	0.032	0.010	0.010	0.050	0.050
PO_4^{-3}	0.010	0.010	0.008	0.008	0.010	0.010
$C_2O_4^{-2}$	0.008	0.008	0.008	0.008	0.008	0.008
SiO_3^{-2}	0.004	0.004	0.004	0.004	0.004	0.004
MoO_4^-	0.0002	0.0002	0.0002	0.0002	0.0002	0.0002

Note: Average high hydroxyl-ion concentrations and average high nitrate concentration waste streams are denoted as HiOH and HiNO.

The bulk-liquid material balance is written as

$$\frac{\partial C}{\partial t} = D_L \frac{\partial^2 C}{\partial x^2} - v_i \frac{\partial C}{\partial x} - \frac{(1-\epsilon_B)}{\epsilon_B} \frac{\partial \Psi}{\partial t}, \tag{1}$$

where D_L is the axial dispersion coefficient, v_i is the interstitial fluid velocity, ϵ_B is bed porosity, and Ψ is the average concentration in the particle, and

$$\Psi = \frac{1}{V_p}\int_0^{V_p} \epsilon_p \bar{C}\, dV + \frac{1}{V_p}\int_0^{V_p} (1-\epsilon_p)\, q\, dV, \tag{2}$$

where V_p is the particle volume and ϵ_p is the particle porosity.

Film resistance to diffusion is included in the boundary condition, which couples the bulk-liquid material balance to the particle material balance. Thus,

$$\frac{\partial \Psi}{\partial t} = \frac{3}{R_p} k_f (C^b - C^s), \tag{3}$$

where R_p is the particle radius, k_f is the film mass-transfer coefficient, C^b is the bulk-liquid concentration, and C^s is the concentration at the particle surface.

The IE-911 particles are treated as a two-phase porous particle containing a network of liquid-filled pores throughout a solid structure. Diffusion occurs through the liquid-filled pores. The particle material balance is written as

$$\frac{\partial \bar{C}}{\partial t}\left[\epsilon_p + (1-\epsilon_p)\frac{\partial q}{\partial \bar{C}}\right] = \frac{1}{r^2}\frac{\partial}{\partial r}\left[r^2 D_e \frac{\partial \bar{C}}{\partial r}\right], \tag{4}$$

where D_e is the intraparticle effective diffusion coefficient. The effective diffusivity is defined in Froment and Bischoff (1990) as follows:

$$D_e = \frac{\epsilon_P}{\tau} D_m, \tag{5}$$

where τ is the particle tortuosity and D_m is the molecular diffusivity. The ionic diffusivity at infinite dilution for Cs was reported as 2.06×10^{-9} m^2/s (Lide, 1996).

Local equilibrium is assumed everywhere inside the particle between the solid phase and the liquid phase. For SRS wastes, a Langmuir isotherm is used to describe the solid/liquid equilibrium. Thus, at each point in the particle,

$$q = \frac{q_t K \bar{C}}{1 + K\bar{C}}, \tag{6}$$

where q_t is the maximum loading on the solid and K is the Langmuir constant.

The initial conditions and Danckwerts (1953) boundary conditions are

$$@ \quad t = 0, \quad \bar{C} = 0 \quad \forall r \quad \text{and} \quad C = 0 \quad \forall \quad x \neq 0$$
$$\text{and } C = C^0 \quad @ \quad x = 0 \tag{7}$$
$$@ \quad r = 0, \quad \frac{\partial \bar{C}}{\partial r} = 0 \quad \forall \quad x$$
$$@ \quad x = L, \quad \frac{\partial C}{\partial x} = 0$$
$$@ \quad x = 0, \quad D_L \frac{\partial C}{\partial x} = v_i (C - C^0).$$

The axial dispersion coefficient is estimated using the correlation developed by Suzuki and Smith (1972). Latheef et al. (2000) conducted experiments and illustrated for small-scale columns that the Suzuki and Smith correlation was adequate. Hence, it has also been used for the column designs. Since the intraparticle resistance to diffusion is the major resistance to mass transfer, large errors in the coefficient for axial dispersion can be tolerated:

$$\frac{D_L}{D_m} = 0.44 + 0.83 \frac{u}{D_m}, \tag{8}$$

where D_m is the molecular diffusivity in cm^2/s and u is the superficial velocity in cm/s.

The film mass-transfer coefficient is estimated based on the Wilke and Hougen (1945) correlation:

$$k_f = \frac{2.62(D_m u)^{0.5}}{a_p (d_p)^{1.5}}, \tag{9}$$

where a_p is the external surface area of the particles per packed volume and d_p is the particle diameter.

The equations are solved numerically. All spatial derivatives are descritized using orthogonal collocation. In the x-direction or along the axial direction of the column, finite ele-

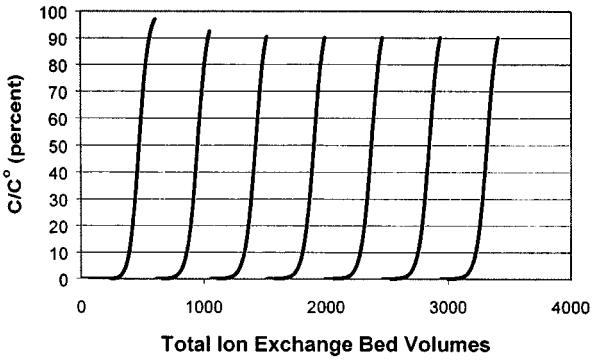

Figure 1. Example of lead column effluent behavior as the carousel system progresses through a series of column switches.

This example is the design simulation for a two-column carousel for an SRS waste labeled HiOH. Flow rate = 1.58 L/s, column diameter = 1.22 m, and column length = 4.88 m.

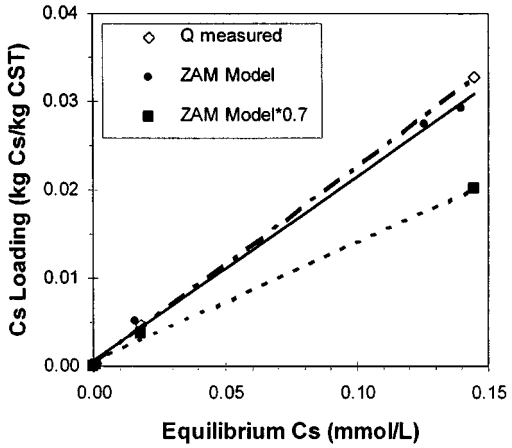

Figure 2. Experimentally measured equilibrium data for the SRS Avg. waste from Walker et al. (1998) vs. predicted data from the ZAM equilibrium model and model values adjusted by a 70% dilution factor.

ments are introduced and Jacobi polynomials are used to approximate the concentration profile in each element. This method allows a large number of collocation points to be used without the numerical oscillation problems typically encountered when high-order polynomials are used. In the *x*-direction, the first derivatives of the concentration profiles were set equal at the boundaries of the elements. In the *r*-direction from the center of the particle, Legendre polynomials were used to approximate the particle concentration profile. The resulting system of algebraic and differential equations was solved using the integration package, DASSL, which is designed to solve systems of this type (Petzold, 1982). Integration is performed using a fifth-order Adams/Moulton algorithm.

The model accounts for the discontinuities in the concentration profile that are introduced when column switches occur. The discontinuities are handled by moving the concentrations at the trailing column collocation points into the collocation points for the lead column and then setting the concentrations at the trailing column collocation points equal to zero, since the trailing column is loaded with fresh CST. By utilizing the procedures illustrated in the following sections to estimate the equilibrium isotherm and the effective diffusivities, a two-column carousel design is presented in Figure 1.

Equilibrium

The equilibrium behavior of the IE-911 granules in the SRS waste was estimated using the previously developed ZAM equilibrium model (Zheng et al., 1997) for the IE-910 powder, which is the commercial powder form of TAM-5. The IE-911 granules are prepared by combining the IE-910 powder with a binder. Thus, a correction factor can be applied to the values predicted from the ZAM model to account for the presence of the binder. This correction can also be used to account for the presence of additional components in actual waste, which are not specifically included in the ZAM model. Based on discussions with SRS personnel, and comparison of predicted distribution coefficients with the ZAM model for the powder, an estimate was made that a particle was effectively composed of about 70% CST and 30% binder. Therefore, the distribution coefficients should be corrected by multiplying the predictions from the ZAM equilibrium model by 0.7. This criterion was later modified.

It should be noted that the carousel design was initially prepared based on preliminary studies, which were used to estimate the equilibrium isotherms and intraparticle diffusion coefficients. This predesign will be referred to as the ''original design.'' Upon completion of some laboratory-scale column experiments at SRS, the original design was modified based on the results of these experiments. Thus, a ''final design'' referred to later was prepared utilizing diffusion coefficients determined from the column experiments.

The preliminary studies had indicated that a 70% correction factor was required for SRS waste to correct for the binder. This 70% factor indicates that the IE-910 powder was diluted by 30% with the addition of a binder. In the design observations presented later, simulations were conducted using the 70% correction for the isotherm. However, recent experimental measurements by Walker et al. (1998) and equilibrium data presented by McCabe (1997) have indicated that the 70% correction factor significantly underestimates the actual IE-911 Cs loading. Figure 2 shows the recently measured data from Walker et al. (1998) along with ZAM model predictions and the model results adjusted by 70%. This graph indicates that no correction factor is required for the ZAM model-predicted values. Interpretation of the data also suggests that a linear isotherm might be used for the design, but one will note that in Table 1, the range of cesium concentrations to be considered are five times the highest measured value presented in Figure 2. The need to consider these higher values of cesium concentrations is what requires the need to use the Langmuir isotherm. In the final design for the SRS waste no correction factor was used for the carousel model simulations.

For design purposes, the SRS waste was subdivided into six categories based on Cs concentration and chemical composition. HiOH, HiNO, and Avg. represent three different chem-

Table 2. Isotherm Parameters for the Six SRS Waste Simulants Compositions

Waste	*qt* (kg/kg)	K (m^3/mol)
Avg.—nominal	0.0771	4.11
Avg.—bounding	0.0771	2.63
HiOH—nominal	0.0770	5.00
HiOH—bounding	0.0770	3.36
HiNO—nominal	0.0771	3.49
HiNO—bounding	0.0770	2.22

Note: Only the nominal compositions of Avg, HiOH, and HiNO were evaluated for the design cases.

ical compositions (see Table 1). The nominal cases represent an average Cs and potassium (K) concentration for each waste, whereas the bounding case represents an upper limit concentration. The ZAM equilibrium model was used to generate equilibrium isotherms for these wastes by varying the Cs concentration while holding the composition of all other components constant. These data were then fit to a Langmuir isotherm. The isotherm parameters are shown in Table 2. No correction factor was applied.

Determining effective diffusivities for SRS waste

In previous studies (Gu et al., 1997; Huckman et al., 1999), batch kinetic experiments were employed to estimate diffusion parameters in IE-911, which were later used to predict column performance. Since such data were not available for the SRS waste, a series of column experiments conducted at Westinghouse Savannah River Technology Center (WSRTC) were conducted. The Avg. SRS waste simulant and three different flow rates were used for the experiments. These experiments were simulated using the two-phase homogeneous column model to estimate a range of possible values for the effective diffusion coefficients. Walker et al. (1998) conducted three column experiments at flow rates of 1.6 CV/h (slow: 0.3 cm/min), 5.9 CV/h (intermediate: 1.0 cm/min), and 22.1 CV/h (fast: 4.1 cm/min). Note that ''CV'' refers to empty column volumes. The experimental parameters for these column runs are presented in Table 3.

Figures 3–5 illustrate the experimental data along with model simulations using the equilibrium isotherms with the parameters presented in Table 2. The ZAM equilibrium model was used to generate cesium loadings for a broad range of equilibrium cesium concentrations. These theoretical data were then used to fit the Langmuir isotherm, and the parameters are presented in Table 2. Effective diffusivities of 0.25, 0.4, and 0.6×10^{-10} m^2/s were used to approximate the

Table 3. Experimental Parameters for Column Runs Conducted at WSRTC

. Parameter	Slow	Intermediate	Fast
Space vel. (CV/h)	1.6	5.9	22.1
Sup. vel. (cm/min)	0.3	1.0	4.1
Col. dia. (m)	0.015	0.015	0.014
Avg. particle dia. (mm)	0.5	0.5	0.5
Col. vol. (L)	0.018	0.018	0.018

Source: Walker et al. (1998).

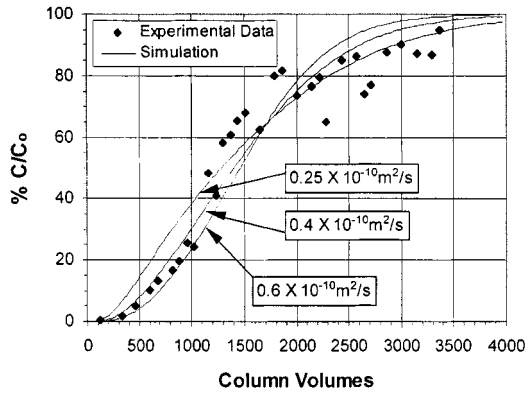

Figure 3. Experimental data for the intermediate run at 5.9 CV/h and model simulations at effective diffusivities of 0.25, 0.4 and 0.6×10^{-10} m^2/s.

breakthrough curves obtained experimentally. The values for the effective diffusivities were considered as the low-limit, best-fit, and high-limit diffusivities, respectively, determined for the ''intermediate'' experiment. These values were then applied to simulate the other experiments. Figure 3 shows the intermediate rate (5.9 CV/h) column experimental data and the three simulations. It is clear that the low-limit value (0.25×10^{-10} m^2/s) provides for a conservative estimate of column breakthrough. Furthermore, the model simulations predicted the solid capacity accurately using the equilibrium isotherm generated from the ZAM equilibrium model and fit to the Langmuir isotherm. One should note the broad scatter in the experimental data; hence one should not expect to estimate the effective diffusivities with less than a 30% and possibly a 50% error.

Figure 4 shows the ''fast'' rate (22.1 CV/h) experiment with the corresponding model simulations. Again, the simulations for the three diffusivities are plotted along with the experimental data. Here the ZAM model predicts a solid loading greater than that indicated by the data. The equilibrium

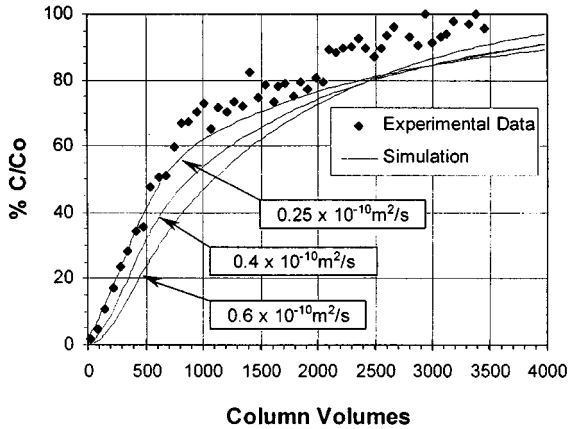

Figure 4. Experimental data for the fast run at 22.1 CV/h and model simulations at effective diffusivities of 0.25, 0.4 and 0.6×10^{-10} m^2/s.

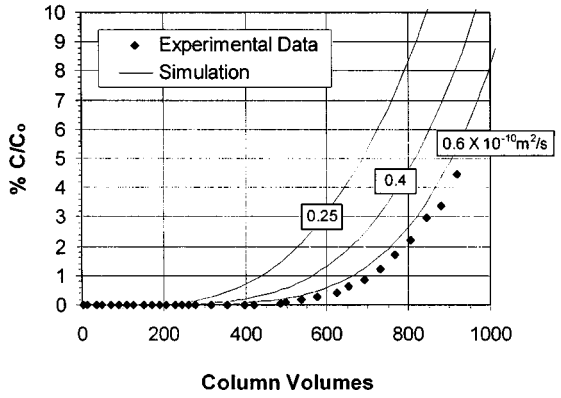

Figure 5. Experimental data for the slow run at 1.6 CV/h and model simulations at effective diffusivities of 0.25, 0.4 and 0.6×10^{-10} m^2/s.

isotherm used was the same for all three runs, since equilibrium capacity is only a function of the simulant composition, feed concentration, and column temperature, which do not differ between these two experiments. One possible reason for the difference may lie in the use of a different IE-911 batch for the fast experiment. Preliminary batch equilibrium studies had indicated a lower loading for the batch used in the fast experiment compared to the IE-911 batch used for the ''slow'' and intermediate runs (Carter, 1999).

Figure 5 shows the experimental data and model simulations for the slow (1.6 CV/h) column run. This plot shows the early part of the breakthrough curve, since the experiment was discontinued at a relative effluent concentration of 4.5%. The simulation at 0.6×10^{-10} m^2/s appears to predict the experimental data well. The best-fit diffusivity would be closer to 1×10^{-10} m^2/s, therefore the value of 0.6×10^{-10} is a conservative estimate for the breakthrough point. The two-phase homogeneous model usually predicts early breakthrough for the IE-911 granules, as indicated from previous studies (Huckman et al., 1999; Latheef, 1999; Latheef et al., 2000).

Design case results

The results for the SRS final design cases are given in Table 4. The primary designs were based on a two-column carousel system with no parallel trains. A conservative effective diffusivity of 0.25×10^{-10} m^2/s is recommended as the design effective diffusivity, although designs are also shown for the higher values of 0.4×10^{-10} m^2/s and 0.6×10^{-10} m^2/s, respectively. The equilibrium parameters were estimated for a Langmuir isotherm using the ZAM equilibrium powder model predictions without any correction factor.

Table 4. Comparison of Previous Design Results for the Two-Column Carousel Using One Minus the Dilution Factors

Waste	D_{eff} (m^2/s) $\times10^{-10}$	1—Dilution Factor	SV (h^{-1})	Interval Time (h)
Avg.	0.2	0.7	0.29	1,750
HiOH	0.2	0.7	0.64	550
HiNO	0.2	0.7	0.26	1,825
Avg.	0.2	1.0	0.29	2,500
HiOH	0.2	1.0	0.64	786
HiNO	0.2	1.0	0.26	2,592

Table 5. Design Results for Fixed Column Diameter (1.22 m) for a Two-Column Carousel with no Parallel Trains

Waste	D_{eff} (m^2/s) $\times10^{-10}$	Length per Col. (m)	Volume Carousel (L)	SV (h^{-1})	Interval Time (h)
Avg.	0.4	4.24	9,910	0.57	1,308
HiOH	0.4	1.97	4,590	1.24	408
HiNO	0.4	4.85	11,330	0.50	1,340
Avg.	0.6	2.93	6,850	0.83	903
HiOH	0.6	1.37	3,200	1.78	283
HiNO	0.6	3.32	7,730	0.73	918
Avg.	0.25	6.68	15,600	0.36	2,060
HiOH	0.25	3.04	7,080	0.80	630
HiNO	0.25	7.59	17,760	0.32	2,104

Note: Lengths are for individual columns and space velocities are based on total carousel volume and feed rate of 1.58 L/s. These results are for the nominal waste solutions.

Table 5 summarizes the results for the three nominal waste compositions.The table shows the required space velocity and the time interval between column switches. Also shown in the table is the design carousel volume based on a feed rate of 1.58 L/s and a length per column based on a column diameter of 1.22 m. Figure 6 shows the results in Table 5 in graphical form. The required volume for a flow rate of 0.95 L/s is 60% of the volume for 1.58 L/s. Thus for cases where the column length is greater than the design specifications, a slower flow rate may be utilized to obtain a shorter column. This situation arose for the large volumes required when a conservative effective diffusivity of 0.25×10^{-10} m^2/s was utilized in preparing the design.

Figure 7 shows the interval time for the column switches for each of the three simulants. The Avg. and HiNO simulants required the greatest volumes, but they also had longer interval times. For the HiOH, however, the required column volume was lower and the change interval was much shorter.

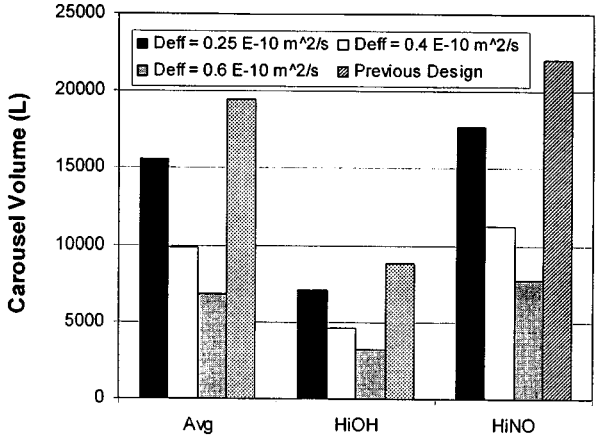

Figure 6. Total volumes for the two-column carousel system for treating SRS waste at 1.58 L/s.

Since the required space velocity does not depend on the flow rate, the volumes required at 0.95 L/s are 60% of the volumes shown in this figure. The previous design values are shown for the 70% correction factor case and $D_e = 0.2\times10^{-10}$ m^2/s.

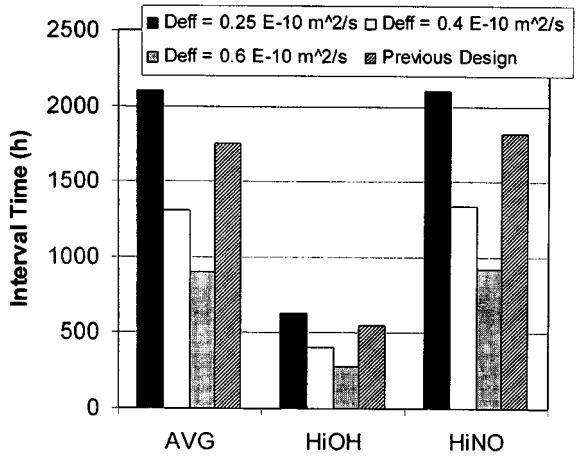

Figure 7. Comparison of column switch intervals for the design cases for the two-column carousel to treat SRS waste.

The previous design values are shown for the 70% dilution factor case and $D_e = 0.2 \times 10^{-10}$ m^2/s.

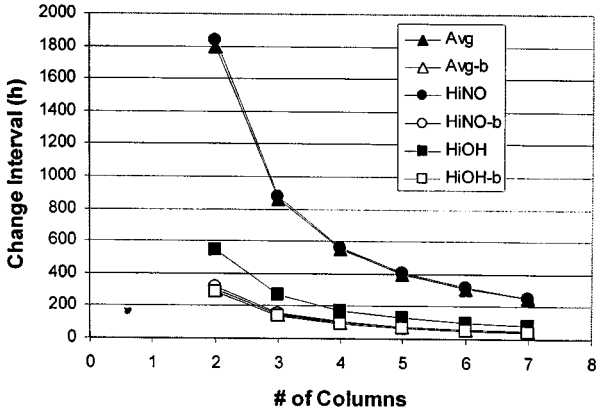

Figure 9. Interval between column switches vs. the number of columns in the system for six waste compositions.

The rate of CST usage is calculated by dividing an individual column volume by the switch interval. This plot is based on the original design using an effective diffusivity of 0.2×10^{-10} m^2/s.

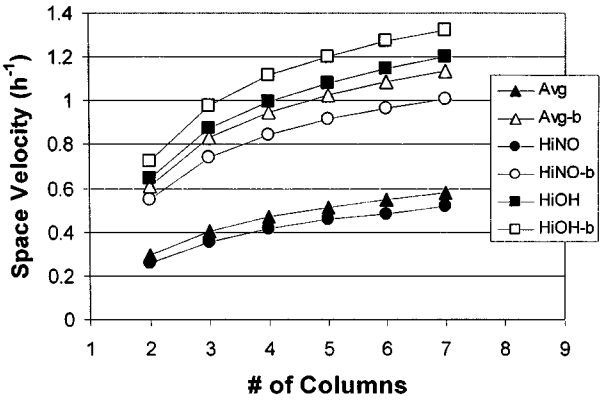

Figure 8. Required space velocity (based on the total carousel volume) vs. the number of columns in the system for six waste compositions.

The worst design case composition is HiNO, which has the lowest space velocity. This plot is based on the original design using an effective diffusivity of 0.2×10^{-10} m^2/s.

Multiple Columns: Effect on Total Carousel Volume and Switching Time

To illustrate how the design volume and the operation of the carousel changes as the number of columns in the carousel changes, carousels were designed with a varying number of columns. Figure 8 shows the space velocity required to meet the design criteria vs. the number of columns in the carousel for six of the waste compositions identified by SRS. The space velocity is based on the total carousel volume. Figure 9 illustrates the interval between column switches. Both Figures 8 and 9 were developed for the original design using an effective diffusivity of 0.2×10^{-10} m^2/s.

From Figure 8 or 9 one can easily visualize the differences in the carousel performance for different waste compositions. The waste composition labeled HiNO requires the smallest space velocity, hence, the largest carousel volume for a given flow rate. The other extreme is the waste labeled HiOH-*b* (bounding) which allows for the largest space velocity, hence, the smallest carousel volume for a given flow rate. These figures indicate the importance of clearly defining the range of possible column feed compositions.

Figures 8 and 9 also illustrate how the total carousel volume required to treat a given waste decreases as the number of working columns in the system increases. The decrease is substantial, moving from two columns to three columns or even from three columns to four columns. For example, the total carousel volume required to treat HiOH decreases by almost 30% when the number of working columns increases from two to three. The decrease becomes more modest as the number of columns increases. The change interval, shown in Figure 9, can become an issue as the number of columns increases because it is reduced to a few days for several of the compositions.

Figure 7 can be used to determine the rate of CST consumption by dividing the volume of an individual column by the switch interval. It is important to note that as the distribution coefficient of a given waste decreases, the amount of CST required to treat that waste increases. Thus, for a given flow rate of waste, a small distribution coefficient implies a large rate of CST usage. However, a large rate of CST usage does not imply that a large ion exchange column is required. In fact, for the waste compositions considered here, those resulting in the lowest distribution coefficients generally require the smallest column sizes. However, the lowest distribution coefficients required more frequent change-out intervals.

The final observation is to illustrate the effect of isotherm nonlinearity on the design carousel volume (Hritzko et al., 2000). As the Cs concentration increases, the isotherm becomes increasingly nonlinear. This nonlinearity decreases the size of the mass-transfer zone. It is also true that as the Cs concentration increases, the distribution coefficient decreases, thus requiring a greater volume of CST. Thus, the

bounding compositions for SRS waste identify the wastes that will require the most CST, but these are the wastes that require the smallest carousel volumes (that is, the largest space velocity).

Conclusions

Several conclusions can be made from the results of this design study. The primary design parameters in determining the ion-exchange column volumes are the effective diffusivities and the shape of the equilibrium isotherms. From the column data presented in Figures 3 through 5, it was clear that a range of effective diffusivities between 0.25 and 0.6×10^{-10} m^2/s approximate the data in a satisfactory manner. The average value of 0.4×10^{-10} m^2/s is within 30% of the true value, which is expected when estimating effective diffusivities from column data. Although a detailed look at the effect of the isotherm was not presented here, previous work by Latheef et al. (2000) and Hritzko et al. (2000) indicate that the shape of the isotherm has an effect on the Cs effective diffusivity for IE-911 breakthrough curves at high concentrations ($>$ 40 ppm Cs).

The design calls for several columns operated in series. The number of active columns determines the CST inventory. From the carousel model simulations, a significant decrease in the inventory occurs when employing three or more active columns in series rather than the two active columns followed by a guard column as specfied by SRS. The actual number of columns used will depend on the total pressure drop allowed for the carousel. Pressure drop was not considered to be a significant factor for the two or three column systems.

Even though the CST inventory required for the carousel is determined by the number of active columns, the total amount of CST required to treat a large volume of aqueous waste is dependent on the distribution coefficient for concentrations of cesium in the waste of less than 1×10^{-5} kg/L. In this low-concentration region, the equilibrium isotherm is nearly linear and the distribution coefficient provides an excellent estimate for equilibrium behavior. Intuitively, for higher concentrations, an effective distribution coefficient can be determined by integrating the Langmuir isotherm from a concentration of zero to the feed concentration and dividing this area by the feed concentration.

Because very long times are required to reach the steady-state mass-transfer zone, the initial columns will experience improved separation that should be accounted for in the carousel model. Figure 1 demonstrates this improved separation, as the initial two columns obtain effluent concentrations greater than 90%.

Acknowledgments

The study conducted at the Department of Chemical Engineering, Texas A&M University, was funded by Westinghouse Savannah River Company under Contract No. AB99788T.

Notation

C = bulk liquid-phase concentration
$\bar{C}$ = pore liquid-phase concentration
C^0 = feed concentration in bulk liquid phase
L = length of reactor
q = solid-phase concentration
r = radial direction to center of particle
t = time
V = volume of liquid
x = spatial direction along length of column

Literature Cited

Alm, A. L., "Final Waste Management Programmatic Environmental Impact Statement," *Tech. Rep.* DOE/EIS-0200-F, Dept. of Energy, Washington, DC (1997).

Anthony, R. G., C. V. Philip, and R. G. Dosch, "Selective Adsorption and Ion Exchange of Metal Cations and Anions with Silico-Titanates and Layered Titanates," *Waste Manag.*, **13**, 503 (1993).

Anthony, R. G., R. G. Dosch, and C. V. Philip, "Method of Using Novel Silicotitanates," U.S. Patent No. 6,110,378 (Aug. 29, 2000); assigned to Texas A&M University System.

Carter, J., personal communication (1999).

Danckwerts, P. V., "Continuous Flow Systems—Distribution of Residence Times," *Chem. Eng. Sci.*, **2**, 1 (1953).

Froment, G. F., and K. B. Bischoff, *Chemical Reactor Analysis and Design*, Wiley, New York (1990).

Gu, D., L. Nguyen, C. V. Philip, M. E. Huckman, R. G. Anthony, J. E. Miller, and D. E. Trudell, "Cs^+ Ion Exchange Kinetics in Complex Electrolyte Solutions Using Hydrous Crystalline Silicotitanates," *Ind. Eng. Chem. Res.*, **36**, 5377 (1997).

Hritzko, B. J., D. D. Walker, and N.-H. Linda Wang, "Design of a Carousel Process for Cesium Removal Using Crystalline Silicotitanate," *AIChE J.*, **46**, 552 (2000).

Huckman, M. E., "Modeling and Performance of TAM-5 CST in Ion Exchange Columns," PhD Diss., Texas A&M Univ., College Station (1999).

Huckman, M. E., I. M. Latheef, and R. G. Anthony, "Ion Exchange of Several Radionuclides on the Hydrous Crystalline Silico Titanate, UOP IONSIV IE-911," *Sep. Sci. Tech.*, **34**, 1145 (1999).

Latheef, I. M., "Ion Exchange Column Studies for the Selective Separation of Radionuclides Using the Hydrous Crystalline Silicotitanate, UOP IONSIV IE-911," PhD Diss., Texas A&M Univ. College Station (1999).

Latheef, I. M., M. E. Huckman, and R. G. Anthony, "Modeling Cesium Ion Exchange on Fixed Bed Columns of Crystalline Silicotitanate (CST) Granules," *Ind. Eng. Chem. Res.*, **39**, 1356 (2000).

Marsh, S. F., Z. V. Svitra, and S. M. Bowen, "Distributions of 14 Elements on 60 Selected Absorbers from Two Simulant Solutions (Acid-Dissolved Sludge and Alkaline Supernate) for Hanford HLW Tank 102-SY," *Tech. Rep.* LA-12654, Los Alamos National Laboratory, Los Alamos, NM (1993).

McCabe, D. J., "Examination of Crystalline Silicotitanate Applicability in Removal of Cesium from SRS High Level Waste," Tech. Rept. WSRC-TR-97-0016, Westinghouse Savannah River Company, Aiken, SC (1997).

Miller, J. E., and N. E. Brown, "Development Properties of Crystalline Silicotitanate (CST) Ion Exchangers for Radioactive Waste Applications," *Tech. Rep.* SAND97-0771, Sandia National Laboratories, Albuquerque, NM (1997).

Petzold, L. R., "A Description of DASSL: A Differential/Algebraic System Solver," Tech. Rep. SAND82-8637, Sandia National Laboratories, Albuquerque, NM (1982).

Suzuki, M., and J. M. Smith, "Axial Dispersion in Beds of Small Particles," *Chem. Eng. J.*, **3**, 256 (1972).

Walker, D. D., W. D. King, D. P. Diprete, L. L. Tovo, D. T. Hobbs, and W. R. Wilmarth, "Cesium Removal from Simulated SRS High-Level Waste Using Crystalline Silicotitanate," *Tech. Rep.* WSRC-TR-98-00344, Westinghouse Savannah River Company, Aiken, SC (1998).

Wilke, C. R., and O. A. Hougen, "Mass Transfer in Flow of Gases Through Granular Solids Extended to Low Modified Reynolds Numbers," *Trans. Amer. Inst. Chem. Eng.*, **41**, 445 (1945).

Zheng, Z., R. G. Anthony, and J. E. Miller, "Modeling Multicomponent Ion Exchange Equilibrium Utilizing Hydrous Crystalline Silicotitanates by a Multiple Interactive Ion Exchange Site Model," *Ind. Eng. Chem. Res.*, **36**, 2427 (1997).

Manuscript received Dec. 9, 1999, and revision received Dec. 29, 2000.